THE ASTROPHYSICAL JOURNAL, 461:L1–L4, 1996 April 10


# MEASUREMENTS OF STRUCTURE IN THE COSMIC BACKGROUND RADIATION WITH THE CAMBRIDGE COSMIC ANISOTROPY TELESCOPE

P. F. SCOTT, RICHARD SAUNDERS, GUY POOLEY, CRÉIDHE O'SULLIVAN, A. N. LASENBY,
MICHAEL JONES, M. P. HOBSON, P. J. DUFFETT-SMITH, AND JOANNE BAKER
Mullard Radio Astronomy Observatory, Cavendish Laboratory, Madingley Road, Cambridge CB3 OHE, England, UK
*Received 1995 December 14; accepted 1996 February 5*

## ABSTRACT

We have observed a $2° \times 2°$ area of sky at frequencies of 15.5 and 16.5 GHz with the Cambridge Cosmic Anisotropy Telescope (CAT). Comparison with earlier measurements at 13.5 GHz shows that the observed structure at 16.5 GHz arises predominantly from the cosmic microwave background. The broadband power, averaged over spherical harmonic multipole orders between 330 and 680, is $(\Delta T/T) = 2.0^{+0.4}_{-0.4} \times 10^{-5}$, which is consistent with the predictions of a standard *COBE*-normalized, cold dark matter model.

*Subject headings:* cosmic microwave background — cosmology: observations

## 1. INTRODUCTION

One of the major goals of observational cosmology is to discover the power spectrum of initial density fluctuations. These fluctuations lead to the formation of structure in the universe, and thus knowledge of their spectrum is vital for discriminating between different models of galaxy formation. Since the discovery of statistical fluctuations in the cosmic microwave background (CMB) by the *COBE* satellite (Smoot et al. 1992), there have been numerous reports of detections of the fluctuations using ground- and balloon-based experiments (e.g., Clapp et al. 1994; Ganga et al. 1994; Gundersen et al. 1995; Netterfield et al. 1995; Ruhl et al. 1995; Cheng et al. 1996) and, in at least one case (Hancock et al. 1994), the discovery of real, individual features in the primordial CMB. However, the situation regarding the power spectrum is still confused (see, e.g., Scott, Srednicki, & White, 1994; White, Scott, & Silk 1994), and there is an urgent need for accurate measurements of the fluctuation power on scales from a few arcminutes to a few degrees.

The Cosmic Anisotropy Telescope (CAT) is a three element synthesis telescope, designed as a prototype for a larger instrument, and is able to map the CMB radiation on angular scales between 10′ and 30′ at frequencies between 13 and 17 GHz (Robson et al. 1993). Initial observations at 13.5 GHz of a field centered on ($\alpha = 8^h20^m00^s$, $\delta = 69°00'00''$, 1950.0), "CAT1," have already been reported (O'Sullivan et al. 1995, hereafter Paper I). Having used the Ryle Telescope to subtract discrete sources, we found unambiguous evidence for an excess signal (in CMB and Galactic structures) above the effects of receiver noise and remnant radio source confusion.

In order to separate the CMB and Galactic contributions, we have now made further CAT observations of the CAT1 field at frequencies of 15.5 and 16.5 GHz.

## 2. OBSERVATIONS AND INITIAL DATA REDUCTION

The new observations at 15.5 and 16.5 GHz were made in separate periods between 1994 March and 1995 April using antenna spacings, measured in wavelengths, scaled to be the same as those of the earlier 13.5 GHz measurements, resulting in a synthesized beam with a FWHM of 27′ in right ascension and 34′ in declination. At a frequency of 15.5 GHz, the three horn-reflector antennas have symmetric-Gaussian envelope beams of 1.96° FWHM, scaling with frequency as $\nu^{-1}$. The observing bandwidth is 500 MHz, and the system noise temperature is 50 K. Measurements were made of the total power in two orthogonal polarizations and were confined to nighttime periods. The data were calibrated by daily observations of Cas A; the overall uncertainty in the flux scaling is less than 10%. A combined plot of the amplitudes on the three baselines as a function of time was consistent with a constant rms noise signal except for well-defined periods where the data were clearly affected by weather. Periods during which the amplitudes on *any* baseline regularly exceeded the normal 3 $\sigma$ level were completely excluded from the analysis, representing a loss, on average, of about 40% of the total data. Since the atmospheric signals have a typical coherence time of 10 s (Robson et al. 1994), much shorter than that of the astronomical signals, their effect will be solely to increase the effective noise levels on the maps. In total 370 and 400 hr of data at 15.5 and 16.5 GHz, respectively, were obtained after exclusion of the contaminated periods.

Standard AIPS tasks were used for data reduction, as described in Paper I. The effect of correlator offsets and antenna cross talk was determined to contribute less than 1 mJy to the resultant maps (Paper I). Sixteen 12 hr observations at 15.2 GHz with the Ryle telescope, with a synthesized beam of 30″ FWHM and an rms noise level of 1.5 mJy, were used to map point sources in the CAT1 field, with subsequent monitoring for variability. Data from lower frequency surveys at 4.85 and 1.4 GHz were used, where available, to provide spectral information on the sources. Thirty-one sources, the weakest having a flux density of around 3 mJy, were subtracted from the CAT maps. A cross-correlation of the source-subtracted maps with a reconstructed map of the foreground radio sources showed no significant correlation. The new results are shown in Figure 1*b* and 1*c* (Plate L1), together with the earlier 13.5 GHz data (Fig. 1*a*). The maps each show significant signals. The excess power falls away from the pointing center in a manner consistent with the envelope beam attenuation. At each frequency, the map made by *subtracting* the individual maps for each orthogonal polarization shows no excess power inside the envelope beam, and the noises are simply those expected given the system temperature, i.e., 7 mJy beam$^{-1}$ at 13.5 GHz and 6 mJy beam$^{-1}$ at both 15.5 and 16.5 GHz. This confirms that the excess power is indeed in the

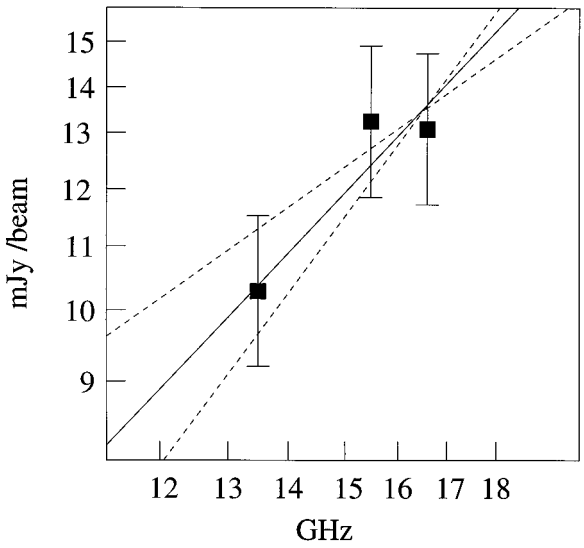


FIG. 2.—A log-log plot of the observed rms powers, after source subtraction, at the three CAT frequencies. The lines represent a least-squares power-law fit, with 1 $\sigma$ limits.

sky. Splitting the total data into two halves, by epoch, yielded the same excess powers, within the errors. The normalized cross-correlation coefficients calculated for the central $2° \times 2°$ area between the map pairs (13.5/15.5 GHz), (15.5/16.5 GHz), and (13.5/16.5 Ghz) are 0.71, 0.66, and 0.67, respectively, implying significant correlation, although a full Monte Carlo analysis of the degree of significance of these figures has not been carried out.

## 3. ESTIMATION OF THE CMB COMPONENT

An indication of the relative magnitudes of the CMB and Galactic contributions can be obtained from a plot of rms power against frequency. Since the *synthesized* beams are almost identical at the three frequencies, the CMB component will have a flux density spectral index of 2, whereas that of the Galaxy can be expected to be between $-1$ and 0. We make a crude estimate of the rms fluctuations in the sky at each frequency by considering the statistics of each map, assuming them to be composed of two random fields, one modulated by the envelope beam, the other not, and fitting amplitudes to each. A least-squares power-law fit to the data gives a value for the spectral index of $1.3 \pm 0.4$. The later analysis (§ 3.1) confirms that most of the emission at 16.5 GHz is due to the CMB. Given this result, we have combined the data from all three frequencies, weighted by $\nu^2$. The combined map (Fig. 1*d*) shows clearly the expected modulation of the CMB signal by the envelope beam. As is apparent from Figure 2, the signal-to-noise ratios are insufficient to perform a pixel-by-pixel spectral separation, in the map plane, of the CMB and Galactic components. We now present a more rigorous analysis of the data.

### 3.1. *Bayesian Analysis*

In order to compare these observations with theory, we adopt the Bayesian approach developed by Hobson, Lasenby, & Jones (1995), which uses the complex visibility data *directly* in the calculation of the likelihood function and thereby removes any need to consider artifacts that may result when these data are Fourier transformed to make a map. This is particularly important when the $(u, v)$-plane is sparsely sampled, as is true for the CAT. The noise levels on the visibilities are deduced from the scatter in these data and will include, for example, errors due to atmospheric effects. Correlated errors between visibilities due to the atmosphere are negligible because of the short period of the atmospheric fluctuations (§ 2), allowing the off-axis terms in the noise covariance matrix to be ignored.

The CAT measures visibilities on loci in the $(u, v)$-plane over a range of baselines between 50 and 110 wavelengths, which corresponds to a range in spherical harmonic multipoles of $l \approx 330-680$. Because of correlations in the $(u, v)$-plane arising from the envelope beam of the antennas, the observed $l$-range can be divided into only two independent bins, which are centered on $l = 410$ and $l = 590$. We therefore split our $(u, v)$-plane sampled by the CAT into two annuli, with widths equivalent to the diameter of the antenna function.

The CMB temperature fluctuations may be expanded in spherical harmonics as

$$\frac{\Delta T(\hat{\mathbf{r}})}{T} = \sum_{l=0}^{\infty} \sum_{m=-l}^{l} a_{lm} Y_{lm}(\hat{\mathbf{r}}),$$

from which we define the CMB power spectrum $C_l = \langle |a_{lm}|^2 \rangle$. We assume that within each bin in $l$-space, the power spectrum of the CMB fluctuations per logarithmic multipole interval is constant, i.e., $l(l+1)C_l = \langle l(l+1)C_l \rangle$ for all multipoles contained in that bin. The derived values represent the average broadband power over the separate $l$-ranges but make no other assumptions about the power spectrum. This approach is obviously more flexible than any method that assumes the form of the power spectrum (or autocorrelation function) for all multipoles.

Regarding foreground signals, we expect the dominant components to be Galactic free-free and synchrotron emission, as well as extragalactic sources that are below our flux limit for subtraction. We assume that the sum of the fluxes from these foreground components may be described by a *single* effective power law $S \propto \nu^{\alpha}$ over the frequency range under consideration, where we expect $\alpha$ to lie approximately in the range $[-1, 0]$. As for the CMB component, the power spectrum of this combined foreground component is also assumed to be constant per logarithmic interval in each bin.

For each bin, the model therefore has three parameters: the broadband powers in the CMB and in the foreground fluctuations and the flux spectral index of the foreground emission. Using the measured visibilities $V$ (and their estimated errors), the likelihood function is evaluated for each bin separately over a wide range in power for each component (sufficient for the likelihood function to go to zero) and over the range $[-1, 0]$ for $\alpha$. By assuming uniform priors for each parameter, the likelihood function is then equivalent to the probability distribution of the parameters given the data in each bin.

Since we have no prior knowledge of the foreground fluctuations, the most conservative estimate of the level of CMB fluctuations is obtained by integrating the probability distribution over the two foreground parameters to give the marginalized probability distribution $\Pr(\langle l(l+1)C_l \rangle | V)$ for the broadband power of the CMB fluctuations in each bin. Confidence intervals are found by integration of this function. Similarly, we integrate over the CMB component and foreground flux spectral index in order to obtain the marginalized probability distribution for the power of Galactic fluctuations in each $l$ bin. Additionally, we can combine the bins and

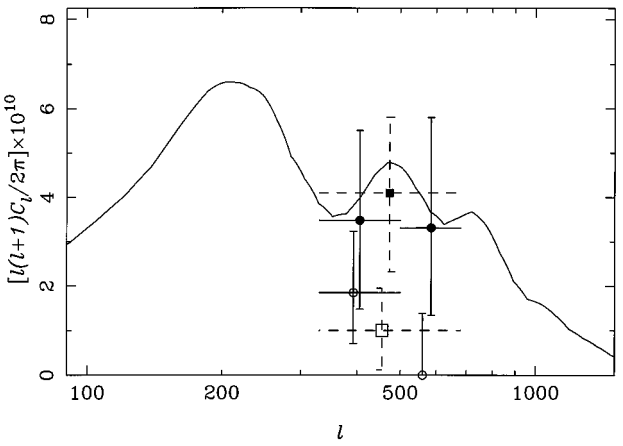


FIG. 3.—Bayesian estimates of the broadband power in the CMB and foreground fluctuations. The filled circles show the power in the CMB in each of the independent CAT bins; the open circles indicate the corresponding power in the foreground component at 16.5 GHz. The vertical error bars show the 68% confidence (1 $\sigma$) points of the probability distributions in each bin; the horizontal lines show the width of each bin. The filled square shows the average CMB power over the entire multipole range to which CAT is sensitive, and the open square shows the corresponding estimate for the foreground component. In each case, the point corresponding to the foreground component has been offset slightly in the interests of clarity. The solid line is the power spectrum predicted by standard CDM with $n = 1$, $h_0 = 0.5$, and $\Omega_b = 0.03$, normalized to the *COBE* result $Q_{\rm rms\text{-}ps} = 20.3$ $\mu$K, assuming $n = 1$ (Tegmark & Bunn 1995).

assume that the CMB and foreground power spectra are constant per logarithmic interval over the *entire* range of multipoles to which the CAT is sensitive, and so estimate the broadband power of each component in a single wide bin, centered on $l \approx 500$.

The results of these analyses are shown in Figure 3. Taking the square root of the broadband power in each bin, we find $\Delta T/T = 1.9^{+0.5}_{-0.5} \times 10^{-5}$ for the bin centered on $l_1 = 410$, and $\Delta T/T = 1.8^{+0.7}_{-0.5} \times 10^{-5}$ for the bin centered on $l_2 = 590$. For the single wide bin centered on $l = 500$, we find $(\Delta T/T) = 2.0^{+0.4}_{-0.4} \times 10^{-5}$. All lower and upper limits correspond to the 68% points of the probability distribution. The total estimated power in both the CMB and Galaxy is consistent with the amount of excess emission observed in the maps. The analysis does not set useful constraints on the value of the foreground spectral index.

## 4. DISCUSSION

The results of Figure 3 show that the Galactic component at frequencies near 15 GHz is small enough, in comparison with CMB fluctuations, for the successful application of the multifrequency approach to foreground rejection which CAT employs. This was expected on the basis of the switched-beam measurements made at 10, 15, and 33 GHz by the Tenerife experiments on 5° scales (Hancock et al. 1994), but it was not clear until now that the extrapolation of this result to smaller angular scales was justified. The implied $l$ dependence of the Galactic component is consistent with previous suggestions of a spatial spectrum $C_l \propto l^{-3}$ (Gautier et al. 1992; Kogut et al. 1996).

The CAT results for the CMB power spectrum displayed in Figure 3 are consistent with the predictions of the *COBE*-normalized, standard cold dark matter model. Detailed testing of cosmological models against the results of this and other experiments must take place in a proper statistical context, taking into account the experiments' differing beam geometries and sampling strategies, etc. This comparison will be carried out elsewhere (Rocha et al. 1996). However, some general remarks can still be made here.

The trend of results from other intermediate scale experiments (with window functions in $l$-space peaking at $l \approx 100$–200) is beginning to support the existence of a "Doppler peak" in this region of $l$-space (White et al. 1994; Hancock et al. 1996), although individual discrepant points are still present. PYTHON II (Ruhl et al. 1995), at $l \approx 90$, gives approximately the same level for $l(l + 1)C_l$ as found in these CAT observations. The CAT measurements, in comparison with these other results, then tend to support the idea that, if indeed there *is* a peak in the power spectrum, it is declining by $l \approx 400$–500. If true, this would be extremely important, for a number of reasons. First, it would indicate that the value of the total density parameter $\Omega$ is close to 1. The value of $\Omega$ controls the angular scale of the CMB fluctuations, with lower $\Omega$ pushing them to smaller scales, and therefore higher $l$. Second, it is now becoming clear (Maguiejo et al. 1996) that, for given cosmological parameters, the power spectrum expected in a cosmic string scenario will have its peak at smaller scales ($l \approx 400$–500) than the peak expected in an inflationary scenario ($l \approx 100$–200). Thus, if the power spectrum really were decreasing by the $l$-range accessible to CAT, this would rule out strings as a viable mechanism for the generation of structure, although the position with respect to textures is less clear. Third, the existence of a peak in the power spectrum on these scales rules out reionization of the universe to any degree that gives significant optical depth back to recombination.

## 5. CONCLUSIONS

The principal conclusions of this paper are

1. the CAT observations at 13.5, 15.5, and 16.5 GHz, after subtraction of radio sources with the Ryle Telescope, reveal excess power in the sky, the structure of which is well correlated between the frequencies;
2. the observed frequency dependence of the excess power is consistent with the bulk of the power at 16.5 GHz being due to the CMB;
3. a Bayesian analysis of the visibility data yields an estimate of $\Delta T/T = 2.0^{+0.4}_{-0.4} \times 10^{-5}$ over the range of multipoles, $l \approx 330$–680, to which the CAT is sensitive;
4. the combination of the new CAT measurements with those from other experiments sensitive to lower $l$ places constraints on the possible values of $\Omega$ and, with increased accuracy over the $l$-range $\approx$90–600, may make it possible to discriminate between the cosmic string and inflationary models for structure formation.

The success of this prototype instrument, operating from a sea level site, confirms the advantages of ground-based interferometers for CMB imaging and power spectrum estimation.

We acknowledge comments from an anonymous referee. We thank the many members of MRAO involved in building and running the CAT. M. P. H. acknowledges a Research Fellowship from Trinity Hall; C. O'S. acknowledges an EU Human Capital and Mobility Fellowship and a PPARC studentship. We gratefully acknowledge PPARC financial support for the CAT.

REFERENCES

Cheng, E. S., et al. 1996, ApJ, 456 L71
Clapp, A., et al. 1994, ApJ, 433, L57
Ganga, K., Page, L., Cheng, E., & Meyer, S. 1994, ApJ, 432, L15
Gautier, T. N., Boulanger, F., Perault, M., & Puget, J.-L. 1992, AJ, 103, 1313
Gundersen, J. O., et al. 1995, ApJ, 443, L57
Hancock, S., Davies, R. D., Lasenby, A. N., Gutierrez de la Cruz, C. M., Watson, R. A., Rebolo, R., & Beckman, J. E. 1994, Nature, 367, 333
Hancock, S., et al. MNRAS, 1996, submitted
Hobson, M. P., Lasenby, A. N., & Jones, M. 1995, MNRAS, 275, 863
Kogut, A., Banday, A. J., Bennett, C. L., Górski, K. M., Hinshaw, G., & Reach, W. T. 1996, ApJ, 460, 1
Magueijo, J., Albrecht, A., Coulson, D., & Ferriera, P. 1996, Phys. Rev. Lett., submitted
Netterfield, C. B., Jarosik, N., Page, L., Wilkinson, D., & Wollack, E. 1995, ApJ, 445, L69
O'Sullivan, C., et al. 1995, MNRAS, 274, 861 (Paper I)
Robson, M., O'Sullivan, C. M., Scott, P. F., & Duffett-Smith, P. J. 1994, A&A, 286, 1028
Robson, M., Yassin, G., Woan, G., Wilson, D. M. A., Scott, P. F., Lasenby, A. N., Kenderdine, S., & Duffett-Smith, P. J. 1993, A&A, 277, 314
Rocha, G., Hancock, S., Lasenby, A. N., & Gutierrez, C. M. MNRAS, 1996, in preparation
Ruhl, J. E., Dragovan, M., Platt, S. R., Kovac, J., & Novak, G. 1995, ApJ, 453, L1
Scott, D., Srednicki, M., & White, M. 1994, ApJ, 421, L5
Smoot, G. F., et al. 1992, ApJ, 396, L1
Tegmark, M., & Bunn, E. F. 1995, ApJ, 455, 1
White, M., Scott, D., & Silk, J. 1994, ARA&A, 32, 319

PLATE L1

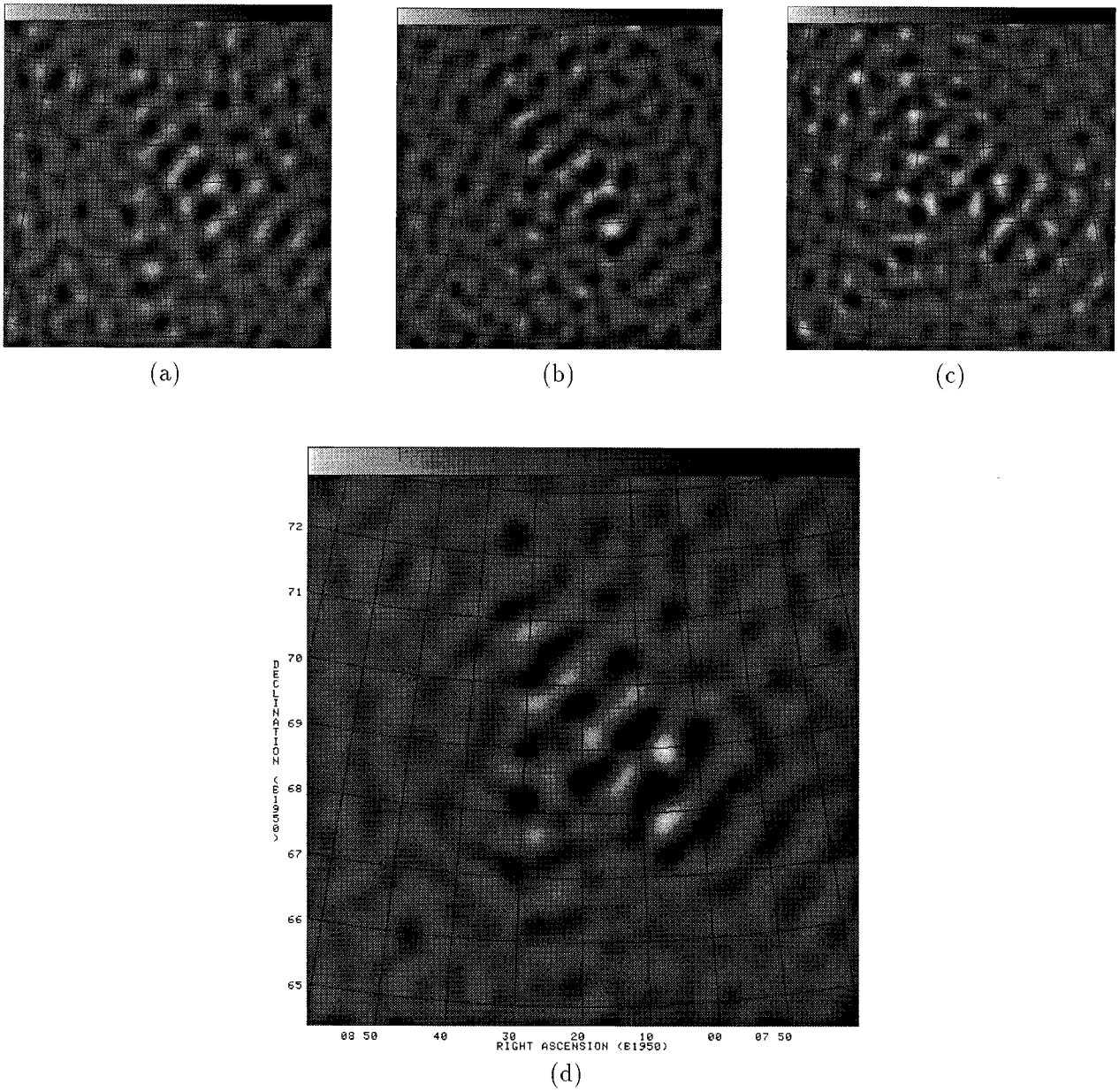


FIG. 1.—(*a*–*c*) Maps of the CAT1 field obtained at 13.5, 15.5, and 16.5 GHz, after point-source subtraction. Each map covers a $6° \times 6°$ area of sky centered on ($\alpha = 8^h20^m00^s$, $\delta = 69°00'00''$, 1950.0). The antenna envelope patterns have a FWHM of about 2°, for which no correction has been applied. The variance near the edge of the maps reflects errors that are due to instrumental and atmospheric noise, which are uniform in magnitude across the map. (*d*) Weighted combination of the three maps. Most of the features on this map are believed to represent CMB structure convolved with the synthesized beam. Gray-scale ranges for the four maps, in mJy beam$^{-1}$, are as follows: (*a*) −34.7–34.5, (*b*) −37.7–36.4, (*c*) −28.9–34.5, and (*d*) −29.7–29.3.